

PACS numbers: 42.50.Ct; 42.50.Gy
DOI: 10.1070/QE2001v031n01ABEH001892

Resonances of coherent population trapping in samarium vapours

N N Kolachevskii, A V Akimov, N A Kiselev, A A Papchenko,
V N Sorokin, S I Kanorskii

Abstract. **Resonances of coherent population trapping were detected in atomic vapours of the rare-earth element samarium. The coherent population trapping was produced by two external-cavity diode lasers (672 and 686 nm) in a Λ-system formed by the three levels of ^{154}Sm: the $4f^6 6s^2(^7F_0)$ ground state, the first fine-structure $4f^6 6s^2(^7F_1)$ sublevel of the ground state and the $4f^6(^7F)6s6p(^3P^o)\,^9F_1^o$ upper level. The dependence of the spectral shapes and resonance contrasts on the polarisation of the laser beams and the direction of the applied magnetic field was studied. The obtained results were analysed.**

Keywords: *coherent population trapping, external-cavity diode laser, high-Q resonances.*

1. Introduction

Coherent population trapping (CPT) is a nonlinear effect produced in a three-level system under the action of two monochromatic light fields, $E_1(t) = E_1 \exp(-i\omega_1 t - i\varphi_1)$ and $E_2(t) = E_2 \exp(-i\omega_2 t - i\varphi_2)$ [1, 2]. Under the Raman resonance conditions, the atomic system is brought to a coherent superposition of internal states that does not interact with the incident biharmonic electromagnetic field. This 'trapping' of the population reduces the absorption of *both* waves. The contrast of the CPT resonance depends, among other things, on the mutual coherence of the waves E_1 and E_2.

The ultimate width of a CPT resonance is determined by the relaxation time of the mutual coherence between the lower levels of the Λ-system and is independent of the width of the upper level because, under the resonance conditions, the incident radiation no longer interacts with it. In the case of appropriatelly chosen long-lived lower levels, one can observe extremely narrow resonances with factors $Q = f/\Delta f$ approaching 10^{14}. So far, most experimental studies of CPT resonances employed alkali atoms, in which the hyperfine-structure components of the ground state, typically split by a few gigahertz, served as the lower states of the Λ-system. The availability of high-precision stable lasers tunable in the region of the resonance transition and the relatively easy phase locking of the light fields E_1 and E_2 have made it possible to detect high-contrast, high-Q CPT resonances in alkali atoms. For example, resonances of width 50 Hz have been detected in caesium atoms [3]. Due to high quality factors of CPT resonances, an atomic system with 'trapped' population can be used as a secondary frequency standard, with the difference of optical frequencies $\omega_1 - \omega_2$ very precisely stabilised [4].

In rare-earth atoms, the distance between fine-structure components of the $4f^n 6s^2$ configuration is typically 10 – 100 THz, which greatly exceeds the hyperfine splitting of the ground state in alkali atoms. The characteristic time of spontaneous decay of these levels, caused by magnetic dipole transitions is a few seconds. The Q factors of CPT resonances in a Λ-system, whose lower levels represent the fine-structure components of a rare-earth atom can potentially be 2 – 3 orders of magnitude larger than those in alkali atoms.

The resonance can be made significantly narrower by increasing the residence time of the atomic system in the laser beams producing CPT. This effect was systematically studied for caesium vapours in neon, which almost does not perturb the coherence of the lower levels of the Λ-system during collisions, increasing the residence time of the Λ-system in the laser beams [3]. The fine-structure levels of the $4f^n 6s^2$ configuration in rare-earth atoms are also weakly sensitive to interatomic collisions because they are well shielded by the external closed $6s^2$ shell [5]. Thus, the potentially high Q factor of CPT resonances in rare-earth atoms opens the prospect of using them in metrological applications, such as secondary frequency standards.

To detect narrow CPT resonances, the laser fields $E_1(t)$ and $E_2(t)$ must satisfy certain phase relations: the medium becomes completly 'transparent' if $\varphi_1 - \varphi_2 = 0$. To satisfy this condition for frequency spacings of the order of 10 THz, one has to employ special techniques because there are no sufficiently simple and stable generators in this frequency range. To date, phase locking techniques have been developed for lasers whose frequencies differ by a few tens of terahertz. As an example, we can cite the technique in which the frequency interval is halved while preserving the coherence [6] or the technique that employs a frequency comb created by locked modes of a Ti:sapphire laser [7].

In this paper, we will study samarium atoms, which has zero total moment of the electron shell in the $4f^6 6s^2(^7F_0)$ ground state ($J_g = 0$). The Λ-system $4f^6 6s^2(^7F_0) \rightarrow 4f^6(^7F)6s\,6p(^3P^o)\,^9F_1^o \rightarrow 4f^6 6s^2(^7F_1)$, whose lower levels

N N Kolachevskii, A V Akimov, N A Kiselev, A A Papchenko, V N Sorokin, S I Kanorskii P N Lebedev Physics Institute, Russian Academy of Sciences, Leninskii prosp. 53, 117924 Moscow, Russia
S I Kanorskii Present address: Max-Planck Institute fur Quantenoptik, Hans-Kopfermann-Str. 1, 85748 Garching, Germany

Received 26 June 2000
Kvantovaya Elektronika **31** (1) 61 – 66 (2001)
Translated by I V Bargatin

are the ground state ($|g\rangle$) and the first fine-structure component ($|low\rangle$) of the $4f^6 6s^2(^7F_1)$ configuration with $\Delta\varepsilon_{12} = 293\ \text{cm}^{-1}$ (Fig. 1), is appealingly simple due to the low values of J for the states involved. Transitions to the upper level ($|up\rangle$), $4f^6 6s^2(^7F_0) \rightarrow 4f^6(^7F)6s6p(^3P^o)^9F_1^o$ at $\lambda_1 = 672$ nm and $4f^6 6s^2(^7F_1) \rightarrow 4f^6(^7F)6s6p(^3P^o)^9F_1^o$ at $\lambda_2 = 686$ nm, are induced by two tuneable diode lasers. The study of the Λ-system of stable samarium isotopes with the zero nuclear spin $I = 0$, such as ^{154}Sm and ^{152}Sm, is simplified because there is no hyperfine splitting in these isotopes. CPT resonances in the Λ-system shown in Fig. 1 are studied experimentally for the first time in this work.

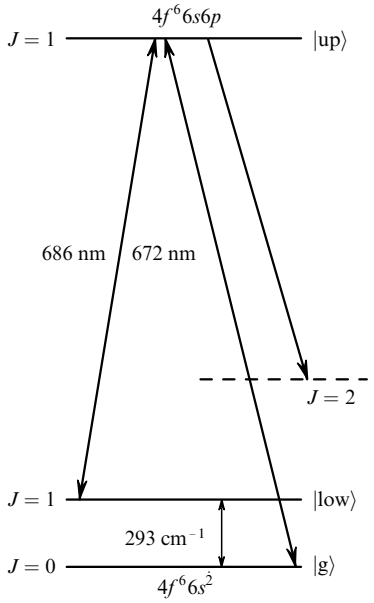

Figure 1. Energy levels of samarium.

2. Coherent population trapping in the Λ-system

Consider the interaction of a Λ-system with two electromagnetic fields $E_1(t) = E_1 \exp(-i\omega_1 t - i\varphi_1)$ and $E_2(t) = E_2 \exp(-i\omega_2 t - i\varphi_2)$, which couple of the long-lived levels $|1\rangle$ and $|2\rangle$ to the upper excited level $|3\rangle$ (Fig. 2), assuming that each field interacts only with one transition. Let us denote the optical frequency detuning by $\delta_L = \omega_1 - \omega_{13}$ and the Raman detuning by $\delta_R = \omega_1 - \omega_2 - \Delta\varepsilon_{12}/\hbar$.

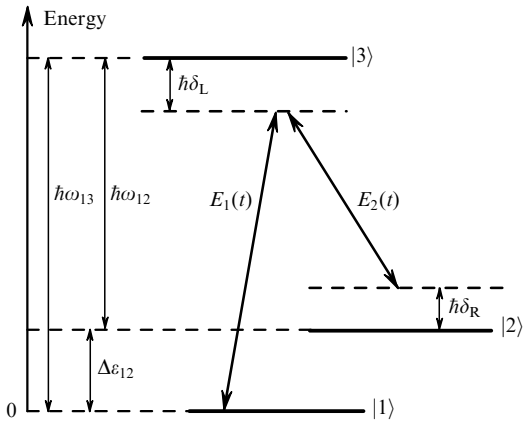

Figure 2. Three-level Λ-system.

If the detunings δ_L and δ_R are small, i.e., the frequencies of waves $E_1(t)$ and $E_2(t)$ are close to the resonance transition frequencies, $\omega_1 \approx \omega_{13}$ and $\omega_2 \approx \omega_{23}$, optical pumping will take place in the system. The system that is excited from the state $|1\rangle$ to the upper state $|3\rangle$ by absorbing a quantum $\hbar\omega_1$ can decay either back to the state $|1\rangle$ or to the state $|2\rangle$, by spontaneously emitting a photon. This results in the increase in the population of the state $|2\rangle$ and hence in the enhancement of the absorption of the field $E_2(t)$ compared to its absorption in the absence of the field $E_1(t)$. The reverse process is also possible when a photon $\hbar\omega_2$ is absorbed resulting in the enhancement of absorption of the field $E_1(t)$. The efficiency of this process increases with increasing population of the state $|2\rangle$. However, 'interference' effects, which appear in the Λ-system with a common upper level in the case of high coherence of laser fields, can reduce the absorption of both fields, $E_1(t)$ and $E_2(t)$.

The basic theory of CPT has been developed in several papers; the most complete account to date can be found in review [4]. We will present here a simplified description of this phenomenon in the considered Λ-system ignoring relaxation. The interference effects in the Λ-system can be conveniently described in the basis representing a linear combination of the eigenstates $|1\rangle$ and $|2\rangle$:

$$|+\rangle = \frac{1}{\Omega}(\Omega_1^*|1\rangle + \Omega_2^*|2\rangle),$$

$$|-\rangle = \frac{1}{\Omega}(\Omega_2|1\rangle - \Omega_1|2\rangle),$$

where $\Omega_1 = -d_{13}E_1/\hbar$ and $\Omega_2 = -d_{23}E_2/\hbar$ are the Rabi frequencies of the respective transitions; $\Omega = (|\Omega_1|^2 + |\Omega_2|^2)^{1/2}$; $d_{i3} = -\langle i|r|3\rangle$, $i = 1, 2$. The states $|+\rangle$ and $|-\rangle$ are not eigenstates of the system; their temporal evolution is described by

$$|+\rangle(t) = \frac{1}{\Omega}[\Omega_1^*|1\rangle + \exp(-i\Delta\varepsilon_{12}\hbar^{-1}t)\Omega_2^*|2\rangle],$$

$$|-\rangle(t) = \frac{1}{\Omega}[\Omega_2|1\rangle - \exp(-i\Delta\varepsilon_{12}\hbar^{-1}t)\Omega_1|2\rangle],$$

where we assume the energy of the level $|1\rangle$ to be zero.

Within the rotating wave approximation, the electric dipole operator V that couples the upper and lower states can be written as

$$V = \frac{\hbar\Omega_1}{2}\exp(-i\omega_1 t - i\varphi_1)|3\rangle\langle 1| + \\ + \frac{\hbar\Omega_2}{2}\exp(-i\omega_2 t - i\varphi_2)|3\rangle\langle 2| + \text{c.c.}$$

The expressions for the matrix elements $\langle 3|V|+\rangle$ and $\langle 3|V|-\rangle$, which determine the coupling between the excited state and states $|+\rangle$ and $|-\rangle$, have the form

$$\langle 3|V|+\rangle = \frac{\hbar}{2\Omega}\exp(-i\omega_1 t - i\varphi_1)\Big\{|\Omega_1|^2 + |\Omega_2|^2\exp[-i(\varphi_2 \\ -\varphi_1) - i(\omega_2 - \omega_1 + \Delta\varepsilon_{12}/\hbar)t]\Big\},$$

$$\langle 3|V|-\rangle = \frac{\hbar\Omega_1\Omega_2}{2\Omega}\exp(-i\omega_1 t - i\varphi_1)\big\{1 - \exp[-i(\varphi_2 - \varphi_1) \\ - i(\omega_2 - \omega_1 + \Delta\varepsilon_{12}/\hbar)t]\big\}.$$

If the difference between the optical frequencies $\omega_1 - \omega_2$ coincides with the energy splitting $\Delta\varepsilon_{12}$ of the lower levels

(the Raman detuning vanishes, $\delta_R = 0$) and the condition $\Delta\varphi = \varphi_1 - \varphi_2 = 0$ is satisfied, these matrix elements assume the form

$$\langle 3|V|+\rangle = \frac{\hbar\Omega}{2}\exp(-i\omega_1 t - i\varphi_1), \quad \langle 3|V|-\rangle = 0.$$

The state $|-\rangle$ is not coupled with the upper level. Because this effect was first observed in fluorescence [8], this state was called a 'dark' state. If the system is irradiated by phase-locked fields $E_1(t)$ and $E_2(t)$, the population is pumped from the coupled state $|+\rangle$ to the 'dark' state $|-\rangle$. The system is extremely sensitive to the phase difference between the laser fields: for example, if $\Delta\varphi = \pi$, the state $|+\rangle$ is 'dark' while the state $|-\rangle$ is 'bright'.

In a specially selected Λ-system, the spontaneous decay time of the lower levels can be extremely large (for example, in the case of hyperfine-structure components of the ground state of alkali atoms, it amounts to several thousand years), and their decay can be neglected when considering linewidths of CPT resonances. The experimentally measured linewidth is determined by the stability of the detuning δ_R and the phase difference $\Delta\varphi$, as well as by Doppler broadening, time-of-flight broadening, Stark broadening (due to optical and external fields), broadening caused by inhomogeneous magnetic fields, and collision broadening. In experiments with alkali atoms, one can stabilise $\Delta\varphi$ very precisely, for example, by modulating the intensity of the laser output at the frequency $\Delta\varepsilon_{12}$. When using two independent free-running diode lasers, one can expect to observe CPT resonances a few megahertz wide.

3. Experimental

Two external-cavity diode lasers were tuned in resonance with the transition wavelenghts in samarium: 672 nm (laser 1) and 686 nm (laser 2). The laser cavities were constructed in the Littrow orientation with a collimating aspherical objective and holographic diffraction grating (1800 lines/mm for laser 1 and 2400 lines/mm for laser 2). The output power of laser 1 in the single-frequency regime was 2.5 mW, and that of laser 2 was approximately 12 mW. The typical width of the emission spectrum of such a diode laser was a few megahertz. However, by introducing a feedback in the current or in the angle of the grating rotation, this width can be reduced substantially. For example, this can be done by locking the laser to an external stable high-Q interferometer.

Earlier, we [9] have studied in detail the spectra of transitions of samarium using the methods of sub-Doppler spectroscopy of absorption saturation [10]. In [9] we measured the relative isotopic shifts and the hyperfine-structure splitting of the levels with an accuracy of 1–2 MHz. We have found that the lines of the ^{154}Sm isotope (natural abundance of 22.75 %) are shifted with respect to the spectral lines of ^{144}Sm (3.07 %), ^{147}Sm (14.99 %), ^{148}Sm (11.24 %), ^{149}Sm (13.82 %), ^{150}Sm (7.38 %), and ^{152}Sm (26.75 %) isotopes by more than 1 GHz to the red, allowing us to lock reliably to the transitions of this isotope.

Fig. 3 shows the schematic of our experimental setup. The Sm vapours were contained in a 50 cm-long cell made of stainless steel with glass windows at the cell ends. The cell could be evacuated or filled with buffer gas as required. A tablet of samarium, about one gram in mass, was placed in the centre of the cell. The 15-cm central part of the cell was heated by a coaxial dc-powered ($\sim$ 500 W) heating coil. The residual magnetic field inside the cell was a few fractions of an oersted. The cell was placed inside two orthogonal Helmholtz coils, 30 cm in diameter, that could create longitudinal ($H_{\parallel}$) or transverse ($H_{\perp}$) magnetic fields of up to 20 Oe in the central part of the cell.

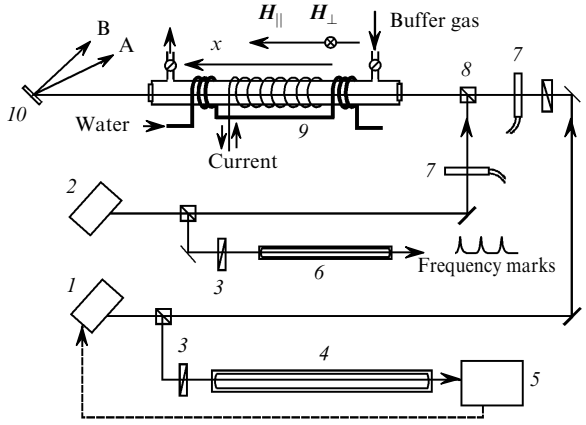

Figure 3. Schematic of the experimental setup: (*1*) laser 1; (*2*) laser 2; (*3*) optical insulator; (*4*) 1 m-long confocal interferometer; (*5*) feedback system; (*6*) 50 cm-long confocal interferometer; (*7*) liquid-crystal modulator; (*8*) polarising beam splitter; (*9*) cell with samarium vapours; (*10*) diffraction grating.

Sm is a relatively high-melting metal (t_m = 1072°C); therefore, we had to heat the cell considerably to produce atomic vapour concentrations that would lead to noticeable absorption. Taking into account that the oscillator strengths of the transitions of interest of us are small ($\sim 10^{-2}$, Table 1) [11] and using the data on the saturated vapour pressure of samarium [12], the necessary concentration can be estimated as $10^{11} - 10^{12}$ cm^{-3}, and the corresponding temperature is 500–600°C. At this temperature, the Doppler width of the transitions under study is $\omega_D/2\pi = 700$ MHz.

Table 1. Oscillators strengths q and transition probabilities Γ.

Transition	Wavelength in the air/nm	$q/10^{-3}$	$\Gamma/10^6$ s^{-1}
$6s^2(J_g = 0) \rightarrow 6s6p\,(J_{up} = 1)$	672.5875	8.5	0.418
$6s^2(J_{low} = 1) \rightarrow 6s6p\,(J_{up} = 1)$	686.0927	9.5	0.449

Table 2 presents the energies and g-factors of the lower metastable states with $J = 0$, 1, 2 and those of the upper level of the Λ-system taken from Ref. [11]. The relative populations of the metastable levels at 600 °C are also given. These levels are thermally populated, and the absorption from the $J = 1$ metastable level is comparable to the absorption from the ground state.

Table 2. Involved levels of Sm.

Even levels $4f^6 6s^2(^7F)$				Odd level $4f^6(^7F)6s6p\,(^3P^o)^9F_1^o$		
J	Energy of the level/cm^{-1}	g	Relative population	J	Energy of the level/cm^{-1}	g
0	0	–	1			
1	292.58	1.50	0.6	1	14863.85	3.10
2	811.92	1.50	0.24			

Laser 1 was tuned in resonance with the $4f^6 6s^2(^7F_0) \rightarrow 4f^6(^7F)6s6p(^3P^o)\,^9F_1^o$ transition in ^{154}Sm, with a small controllable detuning δ_L lying within the Doppler-broadened line shape. We managed to measure the frequency of this transition by using the iodine standard because the iodine line at 14863.9166 cm^{-1}, lies within the detected spectrum of samarium. We have found the frequency of the $4f^6 6s^2(^7F_0) \rightarrow 4f^6(^7F)6s6p(^3P^o)\,^9F_1^o$ transition to be 14863.7305 ± 0.0015 cm^{-1}, improving the accuracy by an order of magnitude with respect to the data of Ref. [11]. Laser 1 was locked to a transmission peak of a stabilised one-meter-long confocal interferometer with low temporal drift (about 5 MHz/hour). The expected linewidth of laser 1 was tens of kilohertz.

Laser 2 was slowly scanned near the $4f^6 6s^2(^7F_1) \rightarrow 4f^6(^7F)6s6p(^3P^o)\,^9F_1^o$ transition so as to cross the point where $\delta_R = 0$. The variation in the laser output frequency was monitored with a half-meter-long confocal interferometer, whose Q factor was approximately 20 and the free spectral range was 149.8 ± 0.1 MHz. According to the measurements [9], the width of the emission spectrum of this laser was approximately 6 MHz. The mode composition of the outputs of lasers 1 and 2 was monitored using a spectrum analyser with a Q factor of 50 and a free spectral range of 8 GHz. To prevent feedback, all interferometers were optically isolated from the lasers.

The linearly polarised beams of both lasers were combined in a polarising cube to form a single beam (with an accuracy of 10^{-3} rad), which illuminated the cell with samarium vapours. The beams were orthogonally polarised, and the vector of the external magnetic field $\boldsymbol{H}_\perp$ lied in the polarisation plane of laser 1. At the cell entrance, the intensities of the beams emitted by lasers 1 and 2 were 0.1 and 0.2 mW mm^{-2} respectively. The beams transmitted through the cell were split by a 1800 lines/mm holographic diffraction grating and entered a two-channel detection system. The signal at 672 nm (laser 1) was detected in channel A, and the signal at 686 nm (laser 2), in channel B. We modulated one of the beams in front of the cell at frequency $f_m = 600$ Hz using a liquid-crystal modulator, and then separated the modulated component from the detected signal of the other beam. In this way, we determined the addition to the absorption induced by the modulated laser beam. We studied the dependence of the spectral shapes on the direction of the magnetic field and the buffer gas pressure.

4. Experimental results

Fig. 4 shows the spectra of the induced absorption detected in channels A and B in the absence of the magnetic field for a buffer gas (argon) pressure of 0.2 Torr. The spectra were detected consecutively, one after the other. In both channels, we observed narrow transmission peaks-CPT resonances. The contrast of these peaks with respect to the total absorption at the line centre was about 5 %. The typical width of the observed CPT resonances, 7 MHz, was mainly determined by the spectral width of laser 2; the inhomogeneity of the laboratory magnetic field also made a small contribution (0.1 MHz).

The CPT resonances were observed against the background of a broad induced absorption band. Consider the typical behaviour of the signal from the frequency-stabilised laser 1 upon scanning the frequency of laser 2. The emission of laser 1 can only interact with those Sm atoms whose velocity projection on the beam axis lies in the interval from v_x to $v_x + dv_x$, where v_x corresponds to the detuning $\delta_L = \omega_{13} v_x/c$ (c is the speed of light). The emission of scanned laser 2 interacts with atoms from another velocity group, $\{v'_x, v'_x + dv'_x\}$, resulting in the increase in the population of the ground state $|g\rangle$ of these atoms due to optical pumping.

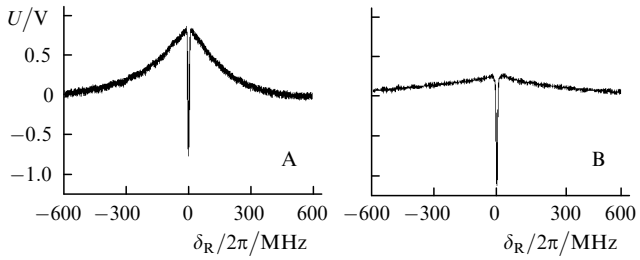

Figure 4. CPT resonance spectra consecutively detected in channels A and B in the absence of a magnetic field for a buffer gas (argon) pressure of 0.2 Torr.

If the mean free path λ_f of atoms, exceeds the diameter D of the laser beam, the absorption at the frequency of laser 1 varies only for $v'_x \approx v_x$, which holds when δ_R is low. If $\lambda_f < D$, collisions results in the transitions of atoms from one velocity group to another. For example, atoms from the velocity group v'_x, which have underwent transitions to the $|g\rangle$ after absorbing a photon of laser 2, can interact efficiently with the beam of the laser 1. This increases absorption of the beam of laser 1 for $|\delta_R| \lesssim \omega_D$.

If Sm atoms collide many times while inside the laser beam, they completely 'forget' their initial velocity group and their velocity distribution becomes Maxwellian. In a gas mixture of samarium and argon, four collisions suffice to do this. An increase in the absorption emission from laser 1 will be determined by the number of atoms contained in the velocity group $\{v'_x, v'_x + dv'_x\}$, i.e., by the Maxwell distribution.

Fig. 5 shows the induced absorption spectra detected in channel A for various buffer gas pressures in the absence of the magnetic field. As pressure increases, the Maxwellian component appears in the absorption band; its maximum shifts to the frequency of the exact resonance, $\omega_2 \approx \omega_{23}$. At pressures of the order of 1 Torr, the shape of absorption band becomes Gaussian with a width of approximately

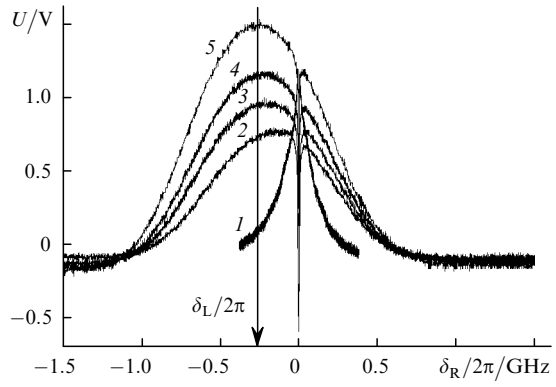

Figure 5. Spectra of induced absorption detected in channel A in the absence of the magnetic field for the buffer gas (argon) pressure of 0.1 (*1*), 0 24 (*2*), 0.77 (*3*), 1.2 (*4*), and 2.0 Torr (*5*).

750 MHz. The band width increases slowly with increasing pressure because the distribution of atom velocities in the initial velocity group becomes closer to Maxwellian, as well as due to the collision broadening of the transition (20 MHz/Torr at room temperature).

The amplitude of the CPT resonance decreases with increasing buffer gas pressure, whereas its FWHM remains constant. In our case, the reduction in the resonance amplitude is caused by the reduction in the life time of atoms in the velocity group $\{v_x, v_x + dv_x\}$, which are resonant with both laser fields. Fig. 6 shows the dependence of the resonance amplitude on the mean free path of Sm in Ar which is normalised to the characteristic diameter of the laser beam ($D = 4$ mm). In our case, the mean free path determines the time required to transfer atoms to the 'dark' state and the CPT resonance amplitude. When the mean free path becomes equal to D, the interaction time is defined by the time of flight through the beam (about 10^{-5} s). Because the transition is only weakly saturated, at the emission intensities used in our experiments [9], the time required for the cyclic $|g\rangle \rightarrow |up\rangle \rightarrow |low\rangle$ transition is of about a few microseconds. Therefore, an atom is excited only a few times as it crosses the beam. An increase in the number of pumping cycles in our unclosed Λ-system will not result in any significant increase in the 'dark' state population because, apart from the transition to the 'dark' state, an atom in the upper state can undergo transitions to the fine-structure component with $J = 2$ (Fig. 1). Thus, an atom that has not been trapped in the 'dark' state, will quickly transfer to the $J = 2$ state and will be lost.

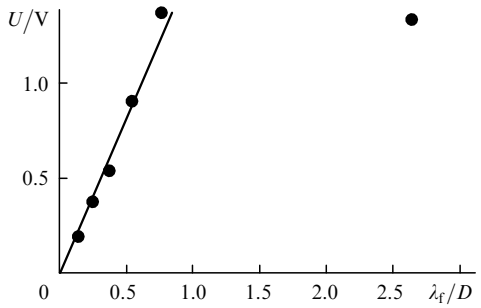

Figure 6. Dependence of the CPT resonance intensity on the mean free path of samarium atoms in argon normalised by the laser beam diameter $D = 4$ mm.

Applying a magnetic field splits the levels into magnetic components and correspondingly changes the shape of CPT resonances. Fig. 7 shows the induced absorption spectra in channel A when a transverse magnetic field $H_\perp = 15$ Oe or a longitudinal magnetic field $H_{||} = 19$ Oe is applied.

If a magnetic field is applied, the ground state $|g\rangle$ remains unchanged ($I = 0$, $J_g = 0$), whereas each of the levels $|low\rangle$ and $|up\rangle$ splits into three magnetic components with $m = -1$, 0, and $+1$. Fig. 8 shows the energy level diagram of the system in a magnetic field (not to scale). In a transverse magnetic field $H_\perp$, the linearly polarised radiation of laser 1 (vector $\boldsymbol{H}_\perp$ lies in the polarisation plane) can induce transitions with $\Delta m = 0$ only (π-components). At the same time, the radiation of laser 2, whose plane of polarisation is perpendicular to $\boldsymbol{H}_\perp$, induces transitions with $\Delta m = \pm 1$ (σ-components).

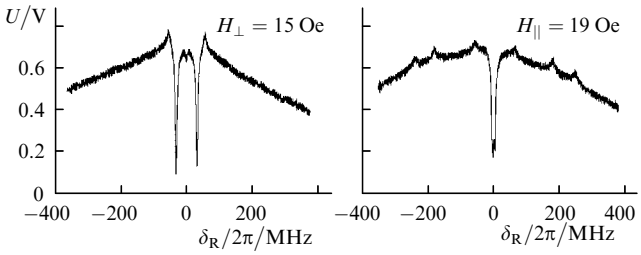

Figure 7. CPT resonances detected in channel A in the case of the transverse magnetic field and the case of the longitudinal magnetic field for the argon pressure of 0.2 Torr.

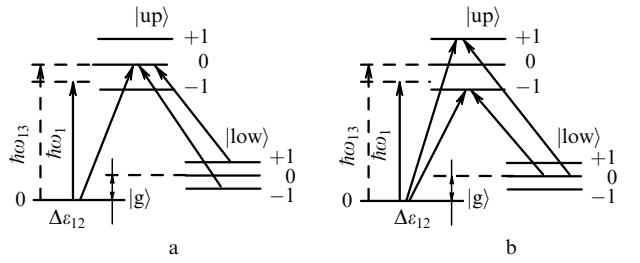

Figure 8. Λ-systems formed in the Sm atom when a transverse (a) or longitudinal (b) magnetic field is applied to the system driven by mutually orthogonal, linearly polarised laser beams.

One can see from Fig. 8a that, in our case, two Λ-systems can be formed with the magnetic quantum numbers of the ground, upper, and lowers states, m_g, m_{up}, and m_{low}, equal to 0, 0, +1 and 0, 0, −1, respectively. Let us determine the conditions for the CPT resonance in these systems. Since in the general case laser 1 is not tuned exactly to the resonance with the transition to the upper level $|up\rangle$, only atoms with a certain projection of the velocity v_x on the beam axis will interact with the radiation of laser 1:

$$\omega_1 = \omega_{13}\left(1 + \frac{v_x}{c}\right).$$

In an atom at rest, the conditions for the CPT resonance correspond to the case $\delta_R = 0$ or the case,

$$\omega_{12} = \omega_{13} - \frac{\Delta\varepsilon_{12}}{\hbar} - \frac{m_{low} g_{low} \mu_B H_\perp}{\hbar},$$

where $g_{low} = 1.5$ is the Lande factor of the metastable state. This condition can be satisfied at two frequencies of laser 2, ω_2^+ and ω_2^-, corresponding to the transitions to the magnetic sublevels with $m_{low} = +1$ and $m_{low} = -1$. Thus, a split CPT resonance line is formed in the spectrum. The splitting coincides with the Zeeman splitting of the lower level,

$$\omega_2^+ - \omega_2^- = -\frac{2 g_{low} \mu_B H_\perp}{\hbar}.$$

In a field of $H_\perp = 15$ Oe, the splitting $\Delta\nu_\perp = |\omega_2^+ - \omega_2^-|/2\pi$ is 65 MHz, which agrees with our estimates.

CPT resonances have a different shape in a longitudinal magnetic field $H_{||}$. In this case, both laser beams can induce transitions with $\Delta m = \pm 1$ only. The corresponding Λ-systems are shown in Fig. 8b. The radiation of laser 1 is in resonance with atoms which have two different velocity

projections, v_x^+ and v_x^-, correspond to magnetic sublevels with $m_{up} = +1$ and $m_{up} = -1$. These velocity projections can be determined from relationships

$$\omega_1 = \left(\omega_{13} + \frac{g_{up}\mu_B H_{||}}{\hbar}\right)\left(1 + \frac{v_x^+}{c}\right),$$

$$\omega_1 = \left(\omega_{13} - \frac{g_{up}\mu_B H_{||}}{\hbar}\right)\left(1 + \frac{v_x^-}{c}\right),$$

where $g_{up} = 3.1$ is the Lande factor of the upper level.

CPT resonances will be observed at two frequencies of the scanning laser,

$$\omega_2^+ = \frac{\omega_1}{\omega_{13}}\left(\omega_{13} - \frac{\Delta\varepsilon_{12}}{\hbar} + \frac{\Delta\varepsilon_{12}}{\hbar\omega_{13}}\frac{g_{up}\mu_B H_{||}}{\hbar}\right),$$

$$\omega_2^- = \frac{\omega_1}{\omega_{13}}\left(\omega_{13} - \frac{\Delta\varepsilon_{12}}{\hbar} - \frac{\Delta\varepsilon_{12}}{\hbar\omega_{13}}\frac{g_{up}\mu_B H_{||}}{\hbar}\right),$$

resulting in the splitting of the CPT resonance line:

$$\omega_2^+ - \omega_2^- = \frac{\Delta\varepsilon_{12}}{\hbar\omega_{13}}\frac{2g_{up}\mu_B H_{||}}{\hbar}.$$

Note the ratio between the CPT resonance splittings in the transverse and longitudinal magnetic fields is

$$\frac{\Delta\nu_\perp}{\Delta\nu_{||}} = \frac{\hbar\omega_{13}}{\Delta\varepsilon_{12}}\frac{g_{low}H_\perp}{g_{up}H_{||}} \approx 25\frac{H_\perp}{H_{||}}.$$

In our case, $H_{||} = 19$ Oe, which corresponds to $\Delta\nu_{||} = 3$ MHz and therefore broadens the CPT resonance (Fig. 7b). Note that, apart from CPT resonances, narrow sub-Doppler peaks of additional absorption are observed in the longitudinal magnetic field at detunings $\delta_R = \pm 1.5\mu_B H_{||}/\hbar, \pm 4.5\mu_B H_{||}/\hbar$, and $\pm 6\mu_B H_{||}/\hbar$.

The Λ-system in the Sm atom is favourably distinguished from complex multilevel systems of alkali atoms by its simplicity and the relative ease of data interpretation (in a magnetic field, the Λ-system of Cs atoms becomes a 48-level system [13]). We believe that the resulting seven-level system can be described analytically. An increase in the time of mutual coherence between the laser beams (e.g., narrowing of the line of laser 2) should result in a significantly increase in the Q factor of the CPT resonances.

Acknowledgements. This work was supported by Volkswagen Stiftung (Grant No. I/73 647), the Russian Foundation for Basic Research (Grant No. 00-15-96586), the program 'Physics of quantum and wave processes' of the Russian Ministry of Science, and the federal program 'Integration' (project AO133 and project 'Mir', participant No. 7).

References

1. Gray H R, Whithley R M, Stroud C R *Opt. Lett.* **3** 218 (1978)
2. Agrawal G P *Phys. Rev. A* **24** 1399 (1981)
3. Wynands R, Nagel A *Appl. Phys. B* **68** 1 (1999)
4. Arimondo E In: *Progress in Optics* (1996) Vol. 35, p. 257
5. Aleksandrov E B, Kotylev V N, Kulyasov V N Vasilevskii K P *Opt. Spektrosk.* **54** 3 (1983) [*Opt. Spectrosc.(USSR)* **54** 1 (1983)]
6. Udem T, Huber A, Gross B et al. *Phys. Rev. Lett.* **79** 2646 (1997)
7. Reichert J, Niering M, Hozwarth R et al. *Phys. Rev. Lett.* **84** 3232 (2000)
8. Alzetta G, Gozzini A, Moi L, Orrios G *Nuovo Cimento B* **36** 5 (1976)
9. Kolachevskii N N, Papchenko A A, Kiselev N A et al. *Opt. Spektrosk.* **90** (2) (2001) [*Opt. Spectrosc.* **90** (2) (2001)]
10. Letokhov V S, Chebotayev V P *Nelineinaya Lasernaya Spektroscopiya Sverchvysokogo Rasresheniya* (Ultrahigh-Resolution Nonlinear Laser Spectroscopy) (Moscow: Nauka, 1990)
11. Martin W C, Zalubas R, Hagan L *Rare-Earth Elements. Atomic Energy Levels* (Washington DC: Institute for Basic Standards, NBS, 1978) p. 162
12. *Tablitsy Fizicheskikh Velichin, Kikoin I S (Ed.)* (Tables of Physical Quantities) (Moscow: Atomizdat, 1976)
13. Wynands R, Nagel A, Brandt S, Meschede D, Weis A *Phys. Rev. A* **58** 196 (1998)